Journal of Atmospheric and Solar-Terrestrial Physics 71 (2009) 175–179

Contents lists available at ScienceDirect

Journal of Atmospheric and Solar-Terrestrial Physics

journal homepage: www.elsevier.com/locate/jastp

Low-latitude gyrotropic waves in a finite thickness ionospheric conducting layer

V.M. Sorokin [a,*], I.Yu. Sergeev [a], O.A. Pokhotelov [b]

[a] *Institute of Terrestrial Magnetism, Ionosphere and Radio Wave Propagation (IZMIRAN), Russian Academy of Sciences, 142190 Troitsk, Moscow Region, Russian Federation*

[b] *Institute of Physics of the Earth (IFZ), Russian Academy of Sciences, Moscow, Russian Federation*

ARTICLE INFO

Article history:
Received 20 April 2008
Received in revised form
4 October 2008
Accepted 6 October 2008
Available online 17 October 2008

Keywords:
Gyrotropic waves
Finite depth conductive layer
Low ionosphere
Phase velocity

ABSTRACT

The eigen-modes of electromagnetic waves in the finite depth conductive layer of the low ionosphere are considered. The dispersion properties of a discrete set of ULF waves are found taking into account the effect of their damping. The dependence of these properties on the propagation angle relative to the ambient magnetic field is analysed.

1. Introduction

Recently Sorokin and Pokhotelov (2005) provided the analysis of gyrotropic wave (GW) propagation in the middle-latitude ionosphere. This type of ULF waves was termed gyrotropic after Sorokin and Fedorovich (1982) since they exist in strongly gyrotropic, weakly ionized plasma. The electrons in such plasma are magnetized whereas the ions are not magnetized. In other words, the off-diagonal components of the dielectric tensor (Hall terms) substantially exceed the diagonal terms (Pedersen terms). The relative role of this effect depends on the parameter $1/g$, where $g=(\nu_e/\omega_e)+(\omega_i/\nu_{in})$ and ω_e, ω_i stand for the electron and ion gyrofrequencies, ν_{ab} is the collision frequency of the a specious with the b specious and $\nu_e=\nu_{ei}+\nu_{en}$. In the lower ionosphere there are two basic low-frequency modes. The first one corresponds to the Alfven mode and the second one refers to the gyrotropic mode. A close inspection of the dependence of g on altitude shows that in the lower part of the E-layer $g \ll 1$. At these altitudes the Alfven waves strongly decay whereas the GWs can propagate with the weak damping (Sorokin, 1988). Their phase velocity is of one or two orders smaller than the Alfven velocity. Physically the weak damping of this mode is due to the fact that the Hall current is orthogonal to the applied electric field. In this case the Joule dissipation is insignificant. In the lower ionosphere the GWs are generated by acoustic or electromagnetic impacts that accompany such phenomena as industrial atmospheric explosions, magnetospheric activity, etc. The dispersion relations and impulse wave functions have been obtained in the framework of the model of the thin conductive layer in the low ionosphere. These waves are usually used for the interpretation of various geophysical phenomena that are accompanied by propagation of the ULF electromagnetic (EM) waves along the Earth's surface with the velocities (1–100) km/s. However, in the real conditions the conductive layer has a finite depth. Incorporation of this effect results in the generation of discrete wave modes in addition to the mode that exists in the infinitely thin conductive layer. Sorokin (1987) and Sorokin et al. (2003) using exact analytical solutions found the dispersion relations for these modes in particular case of the field-aligned propagation when the mode damping is neglected. Moreover, the Pedersen conductivity was neglected and the altitude dependence of the Hall conductivity σ_H was interpolated by

* Corresponding author. Tel.: +7 495 330 9902; fax: +7 495 334 0124.
E-mail address: v_sorokin@mtu-net.ru (V.M. Sorokin).

1364-6826/$ - see front matter
doi:10.1016/j.jastp.2008.10.001

the Epstein layer, i.e. $\sigma_H(z) \propto \cosh^{-1}(z/l)$. Note that the absence of Pedersen conductivity precludes the possibility of incorporation of any wave damping. Furthermore, in order to advance the theory and its applications it is necessary to study the dependence of its characteristics on different propagation angles. For practical applications it is important to interpret the lined wave spectra in the frequency range (1–30) Hz observed in Rauscher and Van Bise (1999) during launches and landings of spacecraft, earthquakes and volcano eruptions. In what follows the dispersion relations of eigenmodes propagating under the angle to the ambient magnetic field at low latitudes are obtained. These dispersion relations take into account the damping in the conductive layer of finite depth.

The paper is structures in the following fashion: Section 2 describes the basic equations for considered problem. Dispersion relations for the GWs in the finite depth conductive layer are obtained in Section 3. Our conclusions and discussions are found in Section 4. Finally, Appendix describes the details of our calculations.

2. Basic equations for EM field in the finite depth conductive layer

We consider the ionosphere immersed in the uniform magnetic field **B**. The perpendicular electric field in the conductive layer can be found from the Ampere's and Faraday's laws (cf. Sorokin and Pokhotelov, 2005)

$$\left(\Delta - \frac{1}{c^2}\frac{\partial^2}{\partial t^2}\right)(\mathbf{B}\times\mathbf{E}) - \mathbf{B}\times\nabla(\nabla\cdot\mathbf{E}) = \frac{4\pi}{c^2}\left[\sigma_P\left(\mathbf{B}\times\frac{\partial\mathbf{E}}{\partial t}\right) - \sigma_H B\frac{\partial\mathbf{E}}{\partial t}\right] \quad \text{and} \quad (\mathbf{E}\cdot\mathbf{B}) = 0, \tag{1}$$

where σ_P and σ_H stand for the Pedersen and Hall conductivities and **E** is the wave electric field.

Due to the high mobility of the electrons the parallel ionospheric conductivity is considered much larger than other conductivities, i.e. $\sigma_\parallel \gg \sigma_P, \sigma_H$. Furthermore, the Gaussian coordinate system (x, y, z) is used with the z-axis directed vertically upwards. We note that the displacement current is also taken into account on the right-hand side of Eq. (1). Moreover, the ambient magnetic field **B** lies in the horizontal plane (x, y) under the angle α to the x-axis. The electric conductivities in horizontally uniform ionosphere depend solely on the z coordinate. We assume that all perturbed values depend on space and time as $\propto \exp(\mathrm{i}kx - \mathrm{i}\omega t)$.

In the low-frequency limit, $\omega \ll 4\pi\sigma_{P,H} \approx 10^7\,\mathrm{s}^{-1}$, Eq. (1) reduces to two scalar equations for the y and z components of the electric field

$$\begin{aligned} &\mathrm{i}k\tan\alpha\frac{\mathrm{d}E_y}{\mathrm{d}z} - k^2E_z - \mathrm{i}\frac{4\pi\omega}{c^2}\left(\frac{\sigma_H}{\cos\alpha}E_y - \sigma_P E_z\right) = 0,\\ &\left(\frac{1}{\cos^2\alpha}\frac{d^2}{\mathrm{d}z^2} - k^2\right)E_y + \mathrm{i}k\tan\alpha\frac{\mathrm{d}E_z}{\mathrm{d}z} + \mathrm{i}\frac{4\pi\omega}{c^2}\left(\frac{\sigma_P}{\cos^2\alpha}E_y + \frac{\sigma_H}{\cos\alpha}E_z\right) = 0. \end{aligned} \tag{2}$$

Since $\mathbf{E}\cdot\mathbf{B} = 0$, the x-component of the electric field is connected with the y-component through the relation $E_x = -E_y\tan\alpha$.

The conductive ionosphere is characterized by the boundary conditions that consist of the relations between the tangential component of the electric field and the normal derivative above and below the ionosphere. We will obtain the wave solutions in these regions and substitute them into the boundary conditions which are derived in Appendix (see Eqs. (A.9))

$$\begin{aligned} E_y\left(\frac{l}{2}\right) &= \left[\cosh(ql) - \frac{\kappa_H\sin\alpha}{q\cos^2\alpha}\sinh(ql)\right]E_y\left(-\frac{l}{2}\right) + \frac{\sinh(ql)}{q}\frac{\mathrm{d}}{\mathrm{d}z}E_y\left(-\frac{l}{2}\right),\\ \frac{\mathrm{d}}{\mathrm{d}z}E_y\left(\frac{l}{2}\right) - \frac{\kappa_H\sin\alpha - \mathrm{i}\kappa_P}{\cos^2\alpha}E_y\left(\frac{l}{2}\right) &= \cosh(ql)\frac{\mathrm{d}}{\mathrm{d}z}E_y\left(-\frac{l}{2}\right) + \left(q\sinh(ql) - \cosh(ql)\frac{\kappa_H\sin\alpha}{\cos^2\alpha}\right)E_y\left(-\frac{l}{2}\right). \end{aligned} \tag{3}$$

Since the wave velocity in the magnetosphere substantially exceeds the velocity of GWs in the E-layer, the tangential component of the electric field above the ionosphere satisfies the Laplace equation, i.e. $\Delta E_y = 0$. The same is valid for the insulated atmosphere below the ionosphere. The solution of Laplace equation above and below conductive layer with the depth l is

$$\begin{aligned} E_y &= A_1\exp\left[-|k|\left(z - \tfrac{l}{2}\right)\right], \quad z > \tfrac{l}{2},\\ E_y &= A_2\exp\left[|k|\left(z + \tfrac{l}{2}\right)\right], \quad z < -\tfrac{l}{2}. \end{aligned} \tag{4}$$

3. Dispersion relation for GWs in the finite depth conductive layer

Substituting (4) into (3) and illuminating the constants A_1 and A_2, one finds the dispersion relation for the GWs in the finite depth conductive layer

$$\begin{aligned} &\left[\frac{\kappa_H^2}{\cos^4\alpha} - 2k^2 + \mathrm{i}\kappa_P\left(|k| - \kappa_H\frac{\sin\alpha}{\cos^2\alpha}\right)\right]\tanh l\sqrt{k^2 - \frac{\kappa_H^2}{\cos^2\alpha}} = \left(2|k| - \mathrm{i}\frac{\kappa_P}{\cos^2\alpha}\right)\sqrt{k^2 - \frac{\kappa_H^2}{\cos^2\alpha}},\\ &\kappa_H = \frac{4\pi\omega\sigma_{H0}}{c^2k}, \quad \kappa_P = \frac{4\pi\omega\Sigma_P}{c^2}. \end{aligned} \tag{5}$$

Let us now consider the limiting case of the conductive layer with infinite conductivity. Such layer is characterized by the finite integral $\int_{-\infty}^{\infty}\sigma_H{}^2(z)\,\mathrm{d}z = \sigma_{H0}^2 l = \text{const}$. Passing in Eq. (5) to the limit $l \to 0$ and $\sigma_{H0} \to \infty$ and keeping $\sigma_{H0}^2 l = \text{const}$, one obtains the dispersion relation for the GWs propagating in the thin layer under the angle α to the horizontal magnetic field

$$\omega^2 - 2k^3la^2\cos^4\alpha + \mathrm{i}\omega\nu k^2\cos^2\alpha = 0. \tag{6}$$

The abbreviations in Eq. (6) are (cf. Sorokin, 1988)

$$\begin{aligned} a &= c^2\sigma_{H0}\Big/4\pi\int_{-\infty}^{\infty}\sigma_H^2(z)\,\mathrm{d}z = c^2\Big/4\pi\sqrt{l\int_{-\infty}^{\infty}\sigma_H^2(z)\,\mathrm{d}z},\\ \nu &= c^2\Sigma_P\Big/4\pi\int_{-\infty}^{\infty}\sigma_H^2(z)\,\mathrm{d}z,\\ l &\equiv \int_{-\infty}^{\infty}\sigma_H^2(z)\,\mathrm{d}z\Big/\sigma_{H0}^2. \end{aligned}$$

For $\alpha = 0$ Eq. (6) coincides with that obtained by Sorokin and Pokhotelov (2005) in the limiting case of parallel wave propagation. The Pedersen conductivity of the upper layer provides the wave damping and in the real conditions does not actually influence their phase velocities.

Making use of designations introduced in Eq. (6), from Eq. (5) one finds

$$\left[\frac{\Omega^2}{\xi^2\cos^4\alpha} - 2\xi^2 + i\varepsilon\Omega\left(|\xi| - \frac{\Omega\sin\alpha}{\xi\cos^2\alpha}\right)\right]\tanh\sqrt{\xi^2 - \frac{\Omega^2}{\xi^2\cos^2\alpha}} = \left(2|\xi| - \frac{i\varepsilon\Omega}{\cos^2\alpha}\right)\sqrt{\xi^2 - \frac{\Omega^2}{\xi^2\cos^2\alpha}},$$

$$\Omega = \frac{\omega l}{a}, \quad \xi = kl, \quad \kappa_H = \frac{\omega}{k}\frac{1}{al}, \quad \kappa_P = \frac{\nu\omega}{a^2 l}, \quad \varepsilon = \frac{\nu}{al}. \tag{7}$$

The analysis of spectral characteristics of waves in the layer of finite depth we will carry out for the case when damping is absent. For that in Eq. (7) we assume that $\varepsilon = 0$:

$$\left(\frac{\Omega^2}{\xi^2\cos^4\alpha} - 2\xi^2\right)\tanh\sqrt{\xi^2 - \frac{\Omega^2}{\xi^2\cos^2\alpha}} = 2|\xi|\sqrt{\xi^2 - \frac{\Omega^2}{\xi^2\cos^2\alpha}}. \tag{8}$$

Eq. (8) yields a discrete set of solutions which takes the form $\omega_n = f(k_n, \alpha, n)$, where n is integer, i.e. $n = 0, 1, 2, 3, \ldots$. The dispersion curves for different n, calculated with the help of Eq. (8), are depicted in Fig. 1. The dependence of the phase velocity $v_n = \omega_n/k_n$ as a function of frequency ω is shown in Fig. 2. One sees that for a fixed wavelength $\lambda = 2\pi/k$ the frequency $f = \omega/2\pi$ increases for the waves with the large n. For instance, if the wavelength for the parallel propagation is $\lambda = 60$ km, the corresponding frequencies are $f \approx 1.5$, 2.0, 3.0, 5.0 Hz. The larger the propagation angle α the smaller the frequencies. The

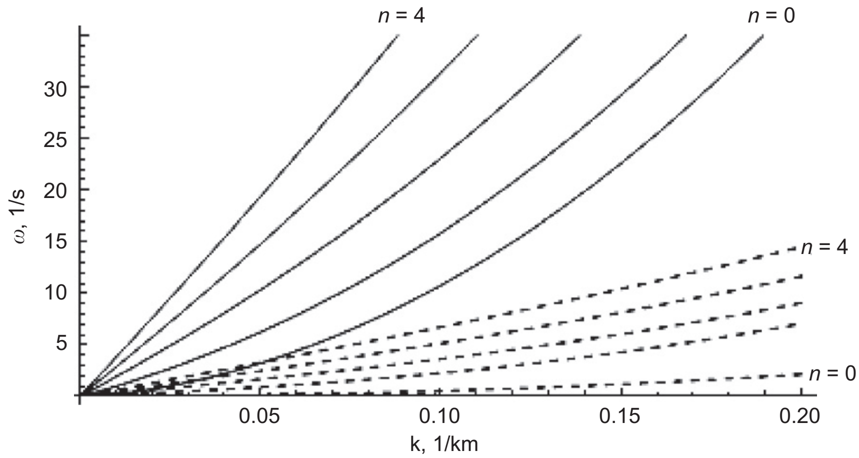

Fig. 1. Dispersion curves for the gyrotropic waves propagating in the finite depth conductive layer under the angel α to the horizontal magnetic field. The Gaussian coordinate system (x, y, z) is used with the z-axis directed vertically upwards. The ambient magnetic field **B** lies in the horizontal plane (x, y) under the angle $\boldsymbol{\alpha}$ to the x-axis. The electric conductivities in horizontally uniform ionosphere depend solely on the z coordinate. Shown are the discrete modes with $n = 0, 1, 2, 3, 4$. The solid line corresponds to $\boldsymbol{\alpha} = 0$, the dashed—$\boldsymbol{\alpha} = 80^\circ$. The parameters used are: $\boldsymbol{\sigma}_{H0} = 8 \times 10^6\,\mathrm{s}^{-1}$, $l = 3 \times 10^6$ cm and $a = 3 \times 10^6$ cm/s.

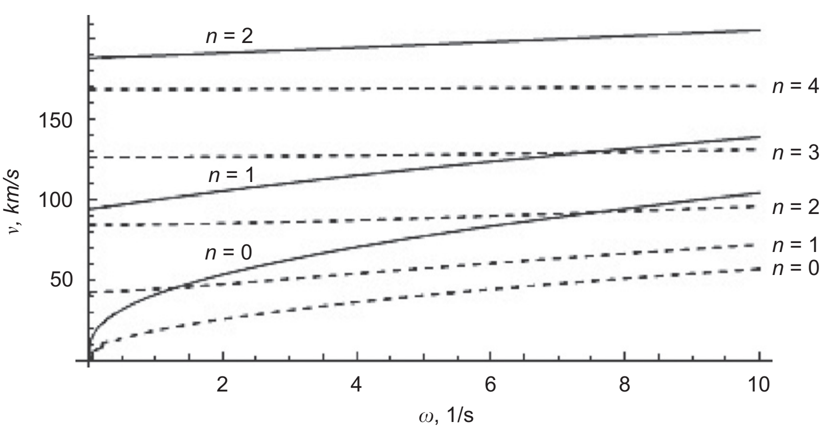

Fig. 2. A plot of the phase velocity $v_n = \omega_n/k_n$ as the function of frequency ω for different discrete modes and different propagation angles. The solid line—$\alpha = 0$, $n = 0,1,2$. The dashed line—$\alpha = 63^\circ$, $n = 0, 1, 2, 3, 4$. Other parameters are the same as in Fig. 1.

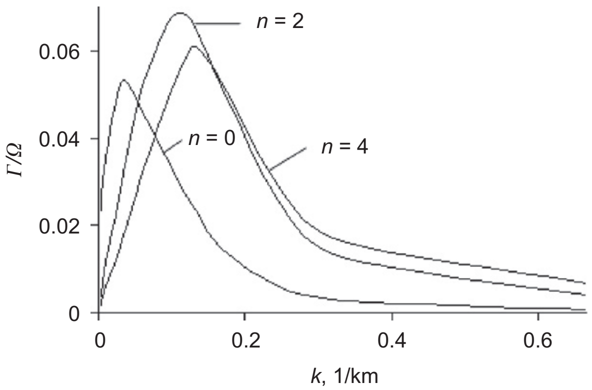

Fig. 3. A plot of normalized damping rate Γ/Ω_1 as the function of the wave number k_n for the discrete gyrotropic wave modes for parallel propagation ($\alpha = 0$). The curves correspond to $n = 0$, 2, 4. The other parameters are: $\sigma_{H0} = 8\times10^6\,\mathrm{s}^{-1}$, $\Sigma_P = 6\times10^6$ cm/s, $l = 3\times10^6$ cm, $a = 3\times10^6$ cm/s and $v = 2\times10^{12}$ cm/s.

phase velocity increases with the increase of the wave frequency or its wave number. The phase velocity of the fundamental mode ($n = 0$) vanishes with the decrease in the frequency. For example, in the frequency range $f = (0\text{–}1)$ Hz for the quasi-parallel propagation the waves with $n = 0$, 1, 2 have the phase velocities that lie in the range $f = (0\text{–}75)$, (90–120) and (190–200) km/s. With the increase in the propagation angle α the phase velocities of each mode decrease.

Let us now consider how the wave damping influences the mode spectral characteristics. Let us now introduce in Eq. (7) the damping rate Γ as $\Omega = \Omega_1 - \mathrm{i}\Gamma$. Fig. 3 shows the normalized damping rate Γ/Ω_1 as a function of the wavelength for the GWs when damping is weak, i.e. $\Gamma \ll \Omega_1$. One finds that maximum damping is attained when $\lambda \approx (30\text{–}100)$ km.

4. Conclusions

It has been shown that in ULF range the conductive ionosphere supports the EM eigen-modes that arise due to the finite depth of the conductive layer. The phase velocity of each mode increases with its frequency and wave number. However, it decreases with the increase in the propagation angle relative to the ambient magnetic field. The dispersion properties of the fundamental mode are basically controlled by a type of the model of the conductive layer. We note that the Pedersen conductivity only influences the value of the phase velocity. It controls solely the wave damping. It was found that the damping attains the maximum value in a specific interval of the mode wavelengths.

Acknowledgements

This research was supported by Russian Fund for Basic Research (Grants no. 07-05-00774, by the Program of the Russian Academy of Sciences No. 16 "Solar activity and physical processes in the Solar-Earth system".

Appendix

We assume the ionosphere consisting of two horizontal conductive layers with different conductivities. The upper layer is characterized only by Pedersen conductivity whereas the Hall conductivity is zero in this region. On the contrary the lower layer is characterized solely by the Hall conductivity and the Pedersen conductivity is zero. The horizontal spatial scale is much larger than the depth of the conductive region. This allows us to consider that inside each layer the conductivity is constant. Assuming in the lower layer $\sigma_P = 0$ from Eq. (2) one obtains

$$\mathrm{i}k\tan\alpha\frac{\mathrm{d}E_y}{\mathrm{d}z} - k^2E_z - \mathrm{i}\omega\frac{4\pi\sigma_H}{c^2\cos\alpha}E_y = 0,$$
$$\left(\frac{1}{\cos^2\alpha}\frac{\mathrm{d}^2}{\mathrm{d}z^2} - k^2\right)E_y + \mathrm{i}k\tan\alpha\frac{\mathrm{d}E_z}{\mathrm{d}z} + \mathrm{i}\omega\frac{4\pi\sigma_H}{c^2\cos\alpha}E_z = 0. \tag{A.1}$$

In the upper layer, assuming$\sigma_H = 0$, from Eq. (2) one obtains

$$\mathrm{i}k\tan\alpha\frac{\mathrm{d}E_y}{\mathrm{d}z} - k^2E_z + \mathrm{i}\frac{4\pi}{c^2}\omega\sigma_P E_z = 0,$$
$$\left(\frac{1}{\cos^2\alpha}\frac{\mathrm{d}^2}{\mathrm{d}z^2} - k^2\right)E_y + \mathrm{i}k\tan\alpha\frac{\mathrm{d}E_z}{\mathrm{d}z} + \mathrm{i}\frac{4\pi}{c^2}\omega\frac{\sigma_P}{\cos^2\alpha}E_y = 0. \tag{A.2}$$

Let us consider the equation for the horizontal component of the electric field in the lower ionosphere layer where the Hall conductivity is nonzero. Illuminating E_z from Eqs. (A.1), one obtains

$$\frac{\mathrm{d}^2E_y}{\mathrm{d}z^2} - \left[k^2 - \frac{4\pi}{c^2}\frac{\omega\sin\alpha}{k\cos^2\alpha}\frac{\mathrm{d}\sigma_H}{\mathrm{d}z} - \left(\frac{4\pi}{c^2}\frac{\omega\sigma_H}{k\cos\alpha}\right)^2\right]E_y = 0. \tag{A.3}$$

The altitude distribution of the Hall conductivity σ_H is approximated by

$$\sigma_H(z) = \sigma_{H0}\eta(z + l/2)\eta(l/2 - z),$$

where $\eta(z)$ is the unit step function. Thus, the vertical derivative in Esq. (A.3) takes the form

$$\frac{\mathrm{d}\sigma_H(z)}{\mathrm{d}z} = \sigma_{H0}[\delta(z + l/2) - \delta(z - l/2)],$$

where $\delta(z)$ is the Dirac delta function. The general solution of Eq. (A.3) inside the layer $-l/2 < z < l/2$ is

$$E_y = C_1\exp(-qz) + C_2\exp(qz),$$
$$q = \sqrt{k^2 - \left(\frac{\kappa_H}{\cos\alpha}\right)^2}, \quad \kappa_H = \frac{4\pi\omega\sigma_{H0}}{c^2k},$$

where C_1 and C_2 are the arbitrary constants. Defining these constants, from above solution one finds

$$E_y\left(\frac{l}{2} - 0\right) = \cosh(ql)E_y\left(-\frac{l}{2} + 0\right) + \frac{\sinh(ql)}{q}\frac{\mathrm{d}}{\mathrm{d}z}E_y\left(-\frac{l}{2} + 0\right),$$
$$\frac{\mathrm{d}}{\mathrm{d}z}E_y\left(\frac{l}{2} - 0\right) = \cosh(ql)\frac{\mathrm{d}}{\mathrm{d}z}E_y\left(-\frac{l}{2} + 0\right) + q\sinh(ql)E_y\left(-\frac{l}{2} + 0\right). \tag{A.4}$$

Integrating Eq. (A.3) over z in the vicinity of upper $z = l/2$ and low $z = -l/2$ planes that bound the layer one finds

$$\{E_y\}_{l/2} = 0, \quad \left\{\frac{\mathrm{d}E_y}{\mathrm{d}z}\right\}_{l/2} = \frac{\sin\alpha}{\cos^2\alpha}\kappa_H E_y\left(\frac{l}{2}\right),$$
$$\{E_y\}_{-l/2} = 0, \quad \left\{\frac{\mathrm{d}E_y}{\mathrm{d}z}\right\}_{-l/2} = -\frac{\sin\alpha}{\cos^2\alpha}\kappa_H E_y\left(-\frac{l}{2}\right). \tag{A.5}$$

In Eq. (A.5) the $\{\ldots\}$ braces denote the difference of the values above and below the corresponding planes, i.e. $\{E_y\}_{l/2} = E_y(l/2{+}0) - E_y(l/2-0)$. Combining the equalities (A.4) and (A.5) one finds the relation between the tangential component of the electric field and its normal derivative at the boundaries of the low ionospheric layer where Pedesen conductivity vanishes, i.e.

$$E_y\left(\frac{l}{2}\right) = \left[\cosh(ql) - \frac{\kappa_H\sin\alpha}{q\cos^2\alpha}\sinh(ql)\right]E_y\left(-\frac{l}{2}\right)$$
$$+\frac{\sinh(ql)}{q}\frac{\mathrm{d}}{\mathrm{d}z}E_y\left(-\frac{l}{2}\right),$$
$$\frac{\mathrm{d}}{\mathrm{d}z}E_y\left(\frac{l}{2}\right) - \frac{\kappa_H\sin\alpha}{\cos^2\alpha}E_y\left(\frac{l}{2}\right) = \cosh(ql)\frac{\mathrm{d}}{\mathrm{d}z}E_y\left(-\frac{l}{2}\right)$$
$$+\left(q\sinh(ql) - \cosh(ql)\frac{\kappa_H\sin\alpha}{\cos^2\alpha}\right)E_y\left(-\frac{l}{2}\right). \tag{A.6}$$

Now let us consider the upper layer of the ionosphere where the Hall conductivity is zero. From Eq. (A.2) one has

$$\left(\frac{d^2}{dz^2} - k^2\right)E_y - \frac{4\pi\omega}{c^2k}\tan\alpha\frac{d}{dz}\sigma_P E_z + \mathrm{i}\frac{4\pi\omega}{c^2}\frac{\sigma_P}{\cos^2\alpha}E_y = 0. \tag{A.7}$$

Assuming this layer to be thin, i.e. $\sigma_P(z) = \Sigma_P\delta(z{-}l/2)$, and integrating Eq. (A.7) one finds

$$\{E_y\}_{l/2} = 0, \quad \left\{\frac{\mathrm{d}E_y}{\mathrm{d}z}\right\}_{l/2} + \mathrm{i}\frac{\kappa_P}{\cos^2\alpha}E_y\left(\frac{l}{2}\right) = 0,$$
$$\kappa_P = 4\pi\omega\Sigma_P/c^2, \tag{A.8}$$

where Σ_P is the height-integrated Pedersen conductivity of the ionosphere. Summing up equalities (A.6) and (A.8), one obtains the relation that connects the tangential component of the electric field and its normal derivative above and below the ionosphere:

$$E_y\left(\frac{l}{2}\right) = \left[\cosh(ql) - \frac{\kappa_H\sin\alpha}{q\cos^2\alpha}\sinh(ql)\right]E_y\left(-\frac{l}{2}\right)$$
$$+\frac{\sinh(ql)}{q}\frac{d}{\mathrm{d}z}E_y\left(-\frac{l}{2}\right),$$
$$\frac{\mathrm{d}}{\mathrm{d}z}E_y\left(\frac{l}{2}\right) - \frac{\kappa_H\sin\alpha - \mathrm{i}\kappa_P}{\cos^2\alpha}E_y\left(\frac{l}{2}\right) = \cosh(ql)\frac{d}{\mathrm{d}z}E_y\left(-\frac{l}{2}\right)$$
$$+\left(q\sinh(ql) - \cosh(ql)\frac{\kappa_H\sin\alpha}{\cos^2\alpha}\right)E_y\left(-\frac{l}{2}\right). \tag{A.9}$$

References

Rauscher, E.A., Van Bise, W.L., 1999. The relationship of extremely low frequency electromagnetic and magnetic fields associated with seismic and volcanic natural activity and artificial ionospheric disturbances. In: Hayakawa, M. (Ed.), Atmospheric and Ionospheric Electromagnetic Phenomena Associated with Earthquakes. Terra Scientific Publishing Company (TERRAPUB), Tokyo, pp. 459–487.

Sorokin, V.M., 1987. Low frequency electromagnetic waves in the lower ionosphere. Geomagnetism and Aeronomy 27, 925–930.

Sorokin, V.M., 1988. Wave processes in the ionosphere related to geomagnetic field. Radiophysics 31, 1169–1180.

Sorokin, V.M., Fedorovich, G.V., 1982. Propagation of the short-period waves in the ionosphere. Radiophysics 25, 495–501.

Sorokin, V.M., Pokhotelov, O.A., 2005. Gyrotropic waves in the mid-latitude ionosphere. Journal of Atmospheric and Solar–Terrestrial Physics 67, 921–930.

Sorokin, V.M., Chmyrev, V.M., Yaschenko, A.K., 2003. Ionospheric generation mechanism of geomagnetic pulsations observed on the Earth's surface before earthquake. Journal of Atmospheric and Solar–Terrestrial Physics 64, 21–29.